Electronic supporting information for

Novel homogeneous photocatalyst for oxygen to hydrogen peroxide reduction in aqueous media

Daniil A. Lukyanov, Liya D. Funt, Alexander S. Konev,* Alexey V. Povolotskiy, Anatoly A. Vereshchagin, Oleg V. Levin and Alexander F. Khlebnikov

**Figure SI1.** UV-Vis absorption spectra of titanyl oxalate – H_2O_2 complex.
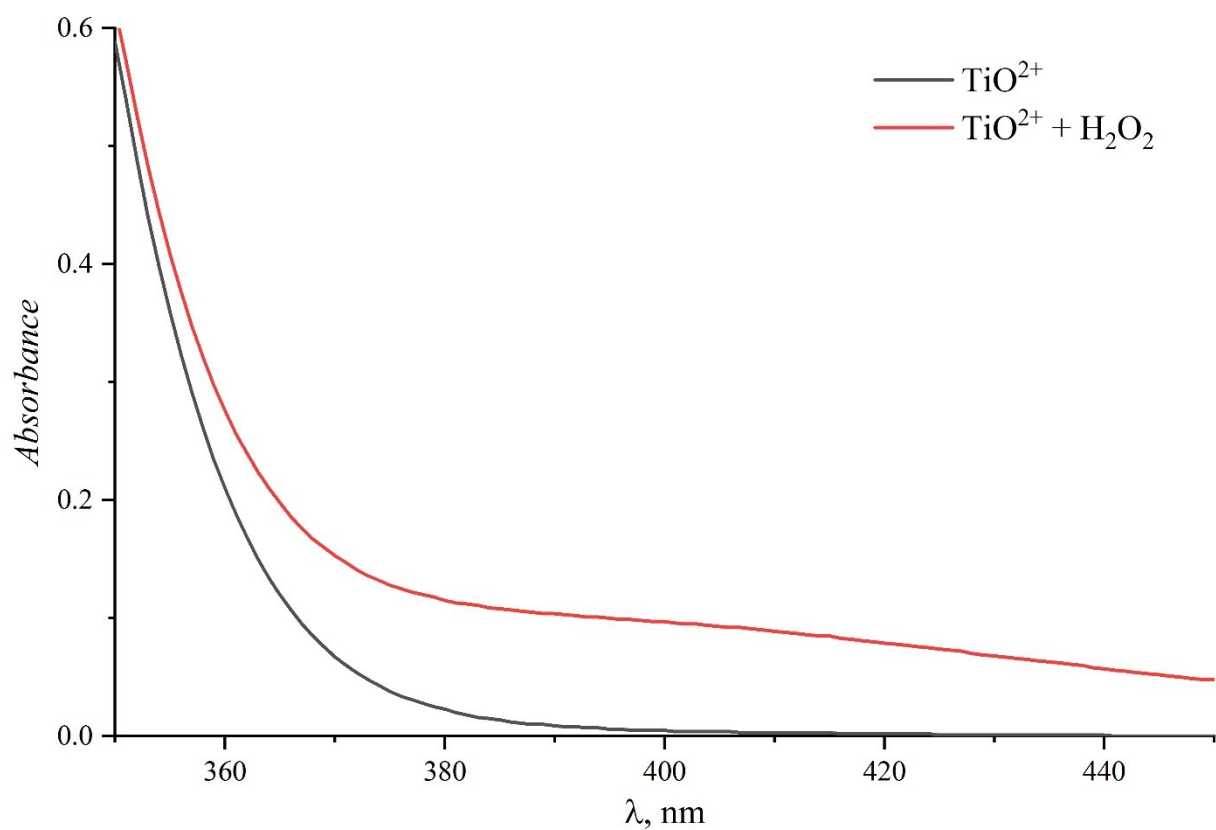
Figure SI2. Calibration curve for titanyl oxalate photometric analysis (absorbance at 400 nm).

$$A = 0.002 + 0.166 \cdot [H_2O_2]$$
$$R^2 = 0.9997$$
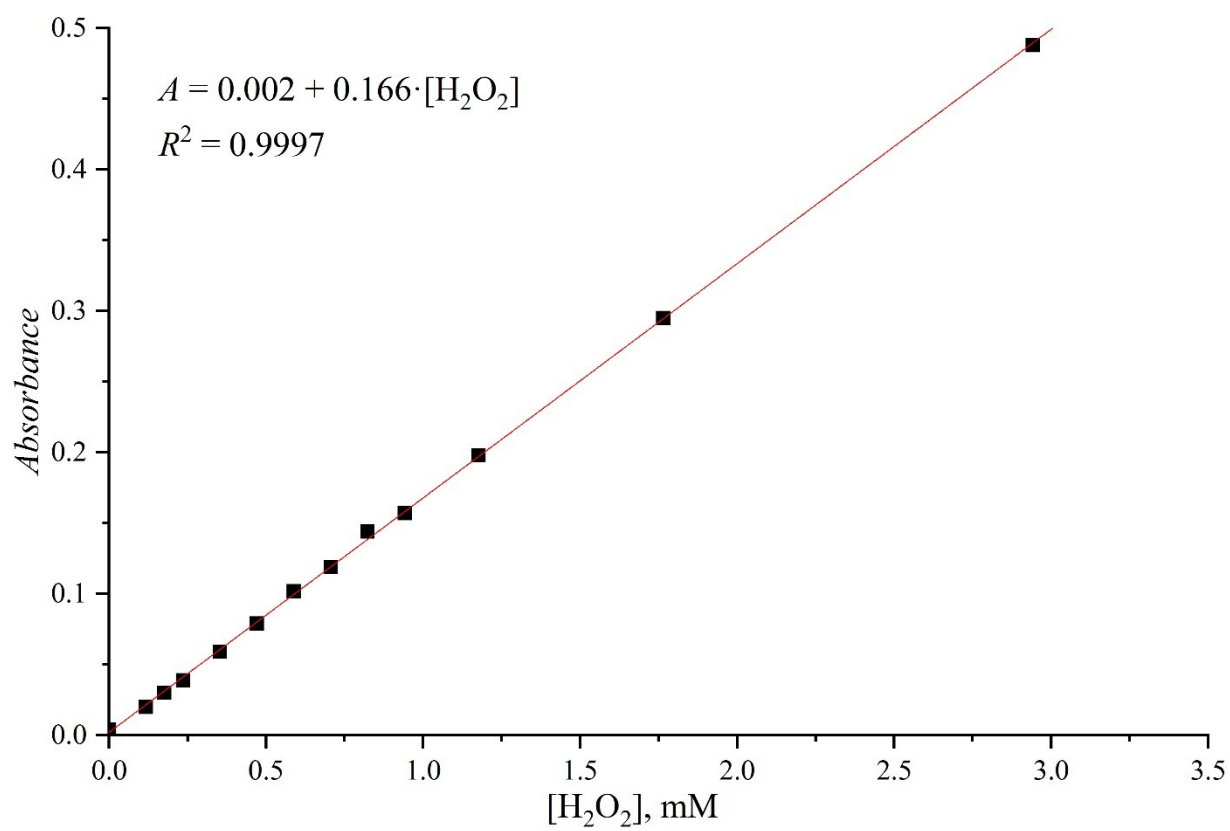
Figure SI3. UV-Vis absorption spectra of **I** (solid line), **IIa** (dashed line) and MeIsoQ (*N*-methylisoquinolinium tetrafluoroborate, dotted line) in water (*c* 0.1 mM).
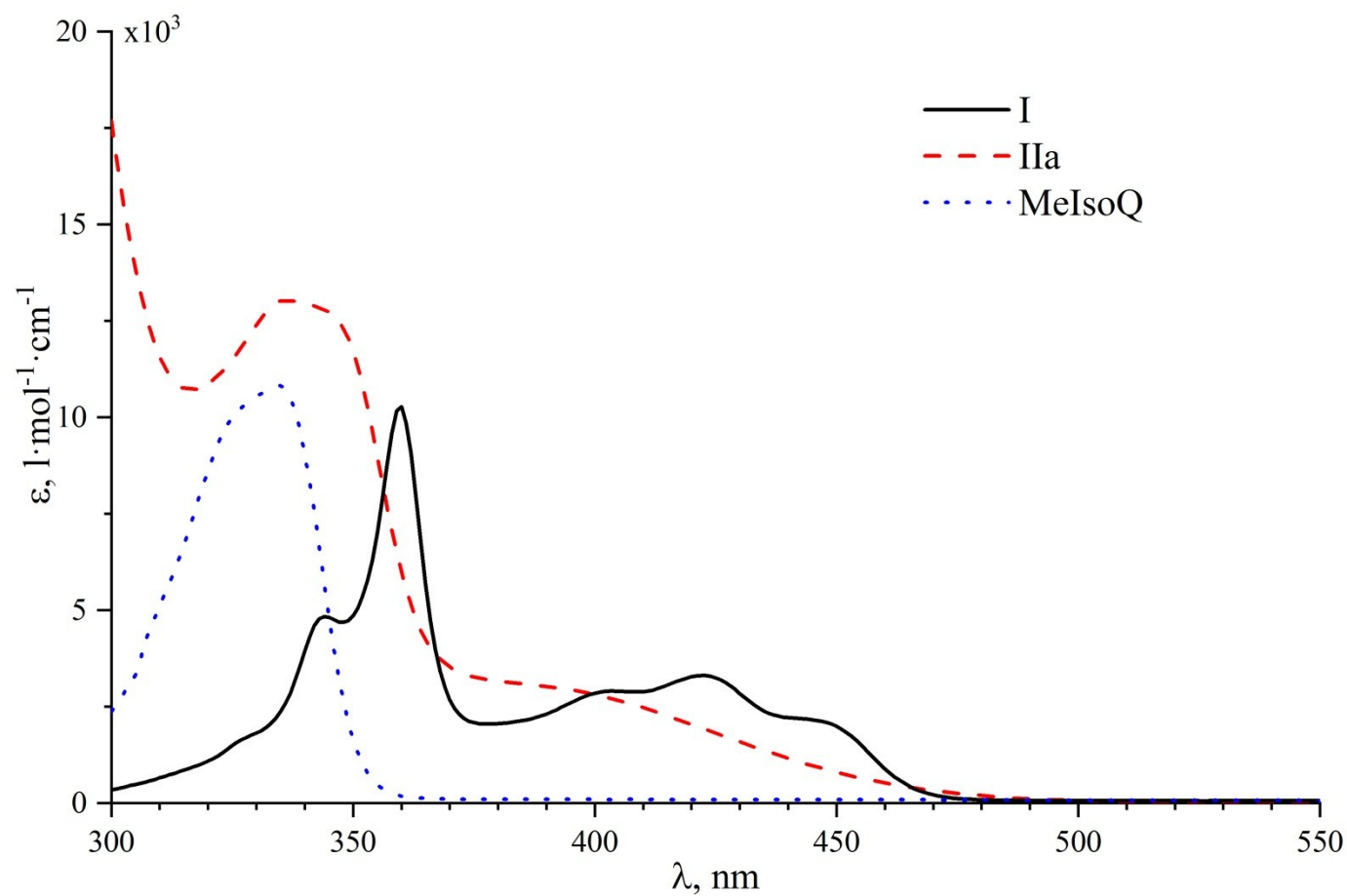
**Figure SI4.** UV-Vis absorption spectra of **IIa-d** in water (*c* 0.1 mM).
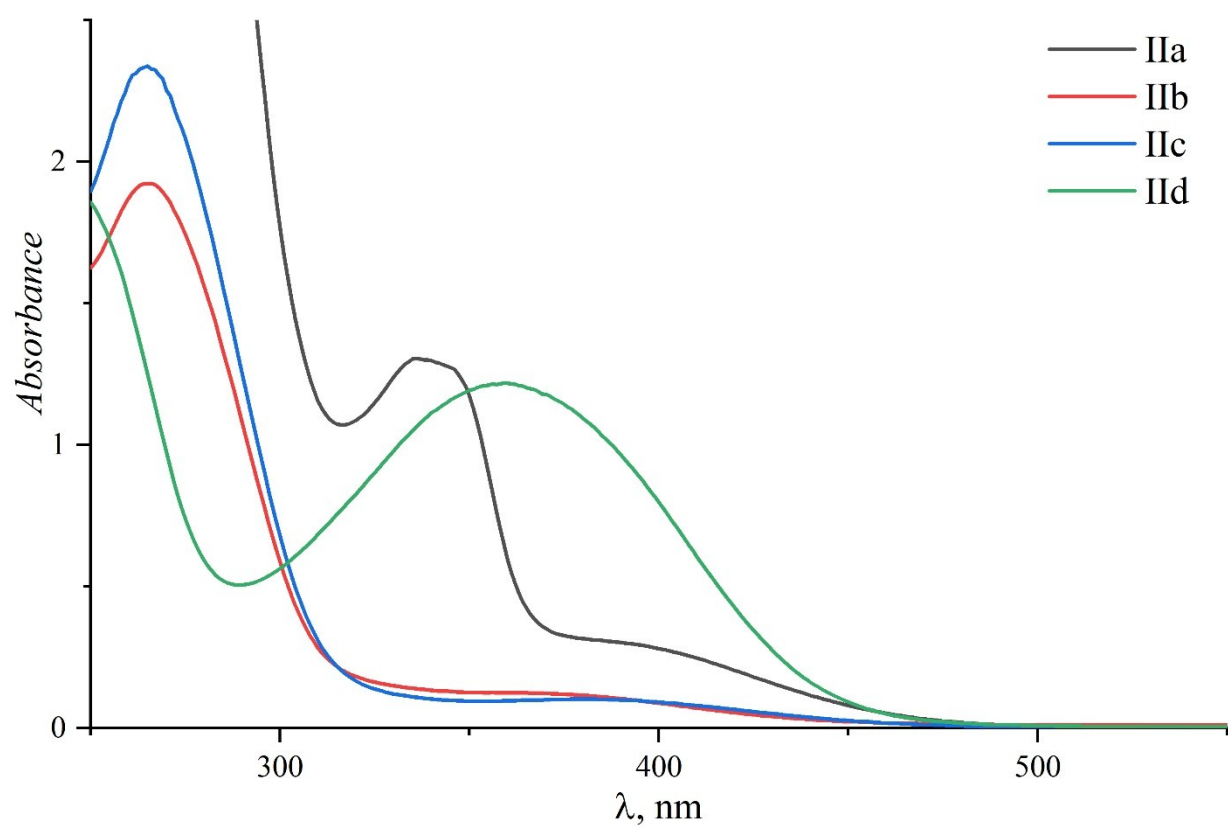
Figure SI5. UV-Vis absorption spectra of **IIIa-d** in water (c 0.1 mM).
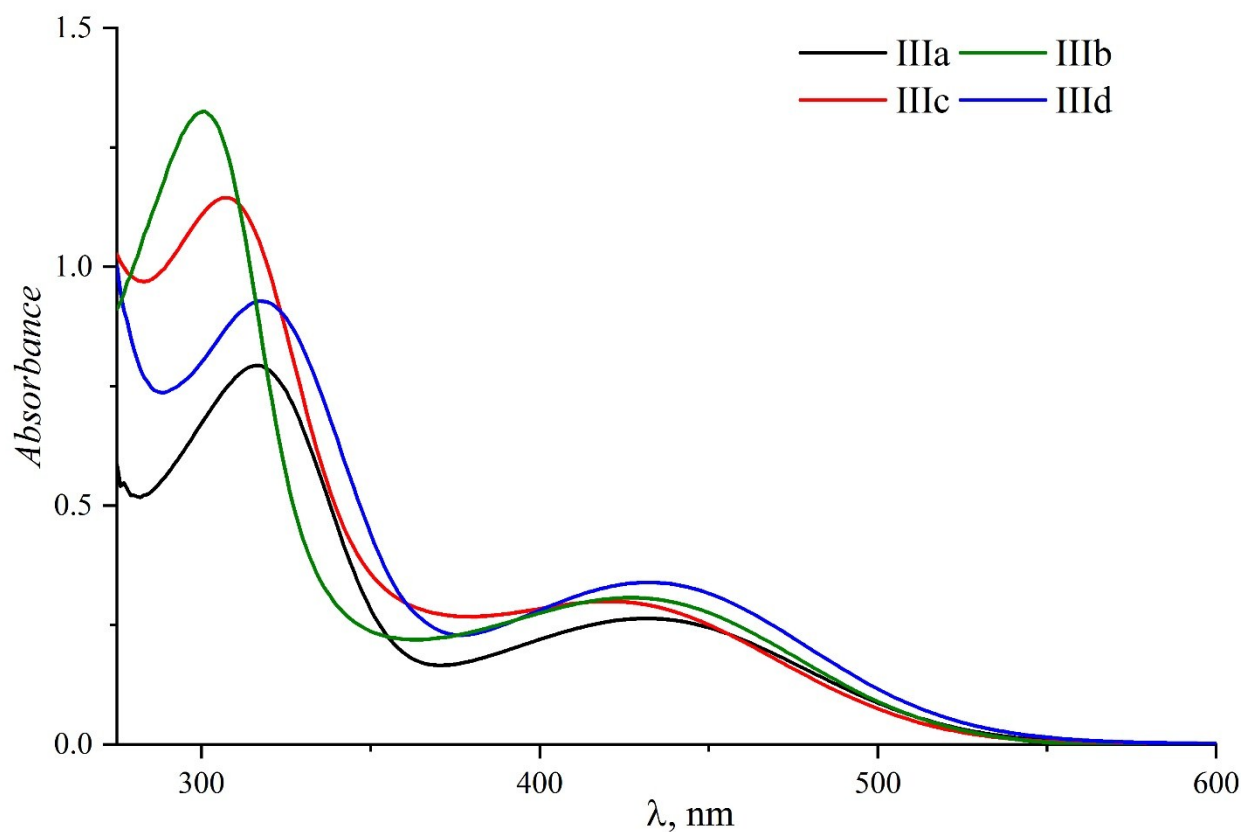
**Figure SI6**. UV-Vis absorption spectra of **IIa** (c 0.1 mM) with titanyl oxalate additive (1 equiv.) in water.
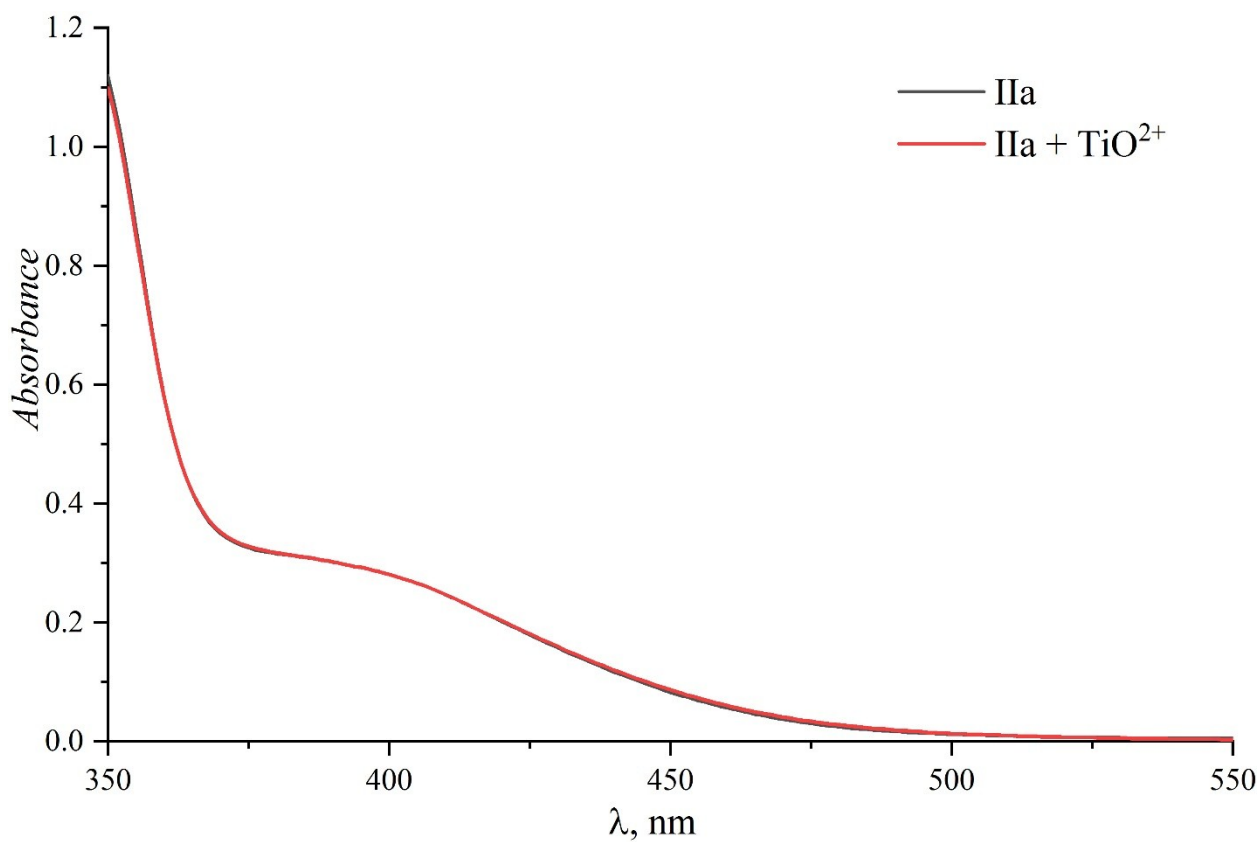
Figure SI7. UV-Vis absorption spectra of **IIIa** (*c* 0.1 mM) with titanyl oxalate additive (1 equiv.) in water.
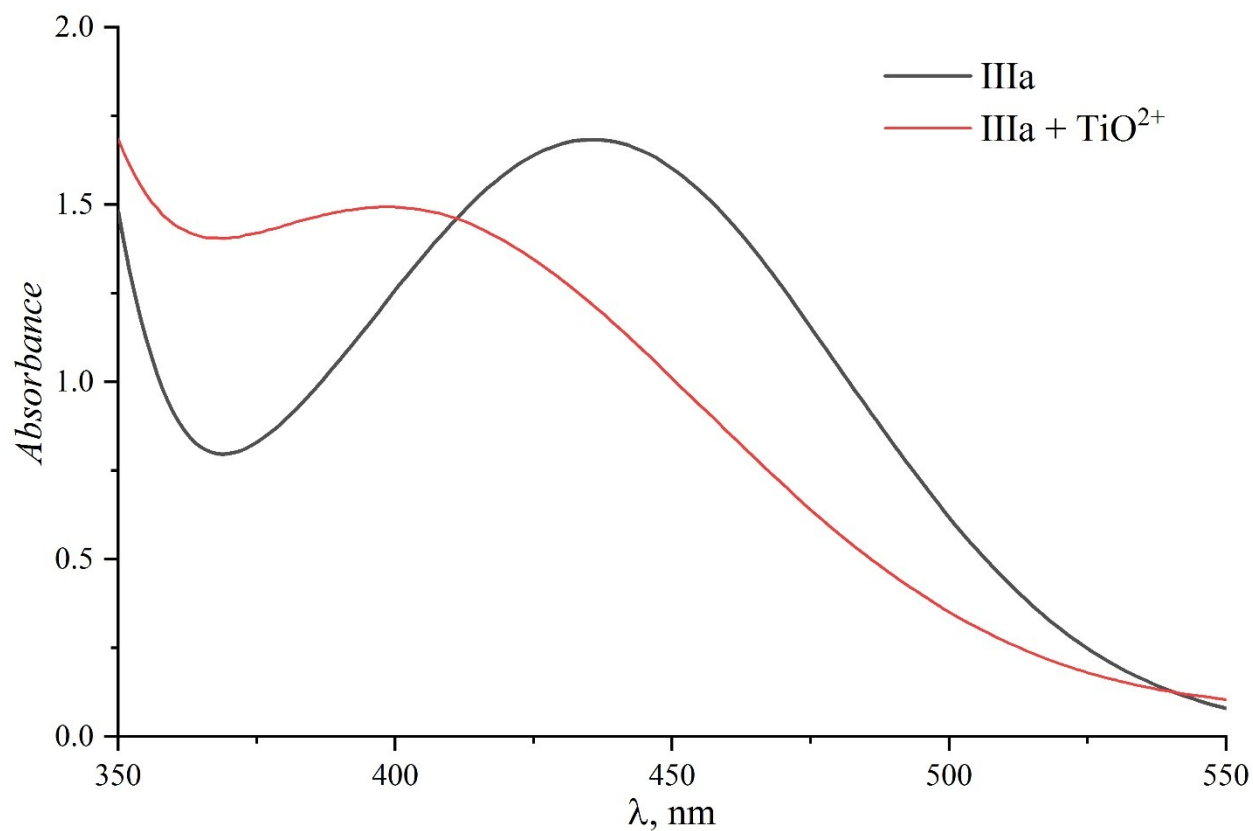
Figure SI8. Increase of the absorbance of the titanyl oxalate H_2O_2 complex upon photocatalytic reduction of O_2 with oxalate photocatalyzed by compound **I**.
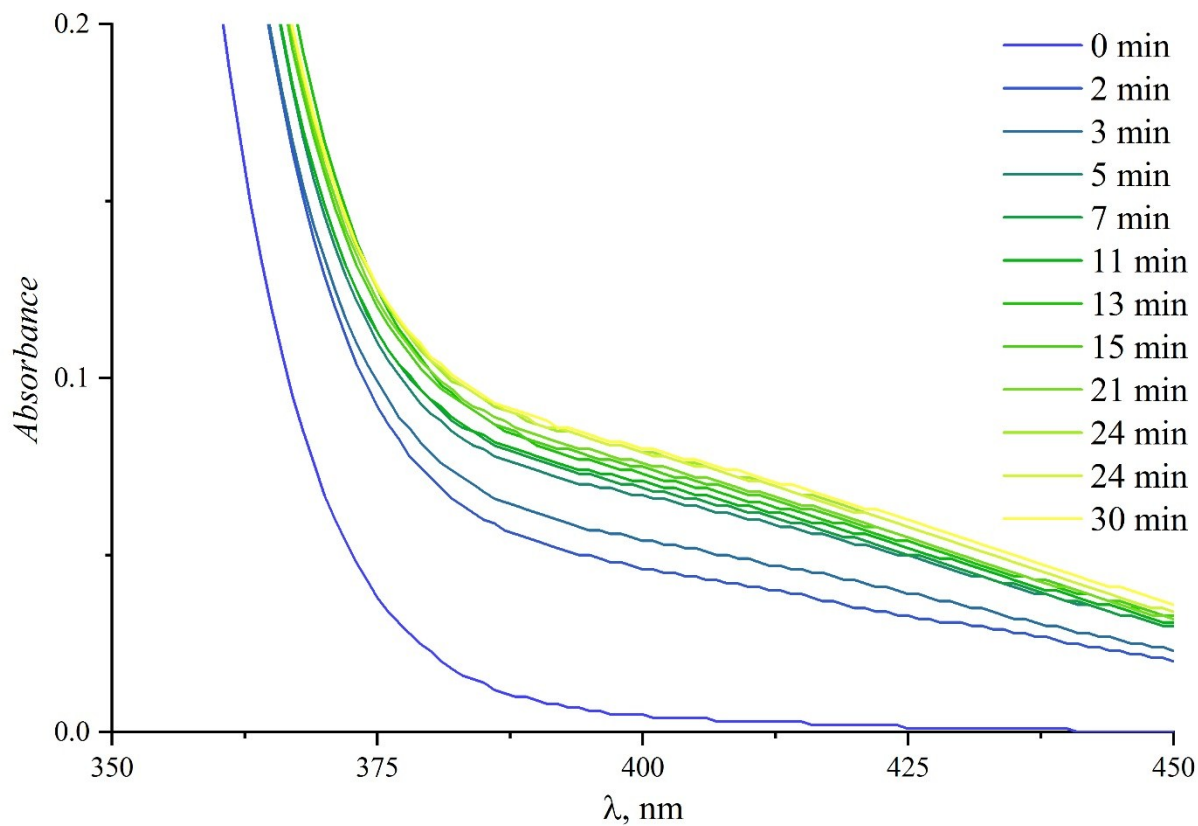
Figure SI9. Increase of the absorbance of the titanyl oxalate H_2O_2 complex upon photocatalytic reduction of O_2 with oxalate photocatalyzed by compound **IIa**.
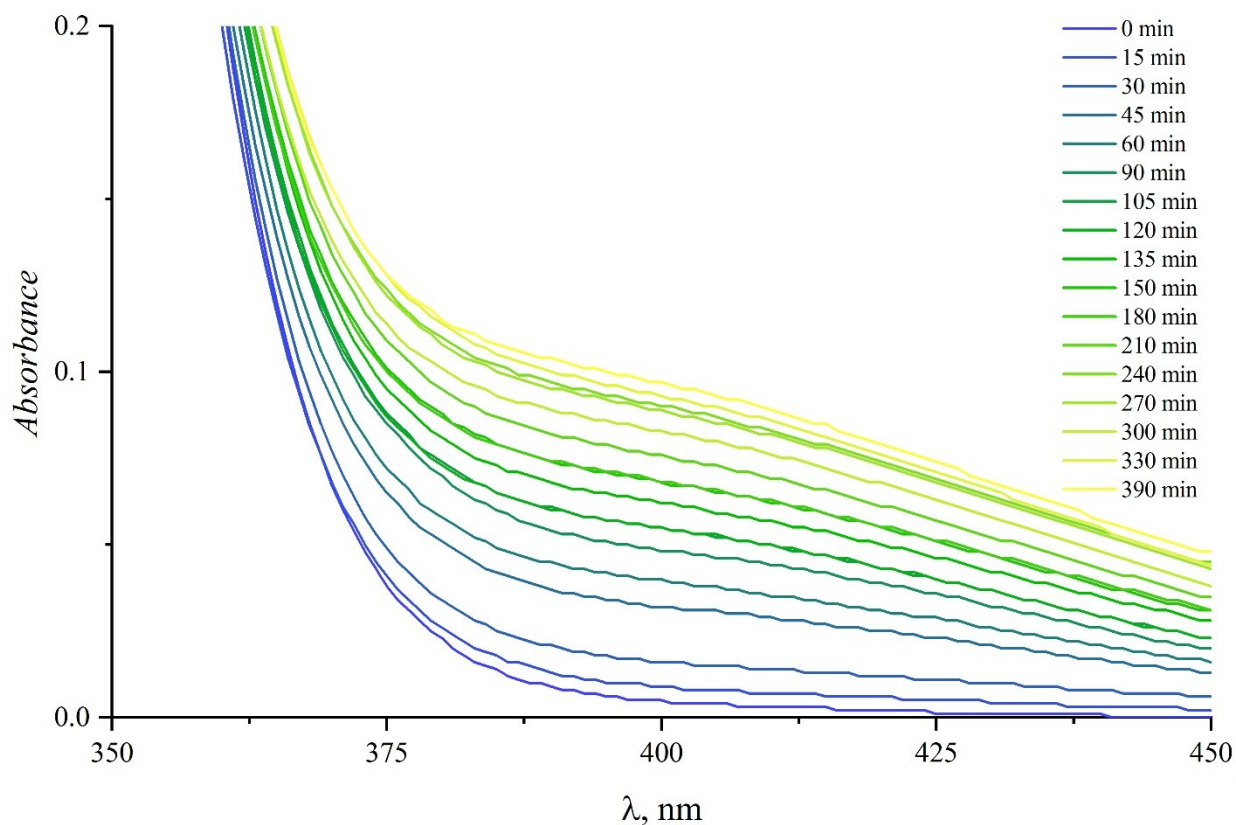
Figure SI10. Control experiments for H_2O_2 generation: without the catalyst (blue line), without irradiation (green line) and irradiation under argon (red line) compared to H_2O_2 generation upon irradiation of the reaction mixture purged with O_2 with 420 nm LED in the presence of **IIa** (black line).
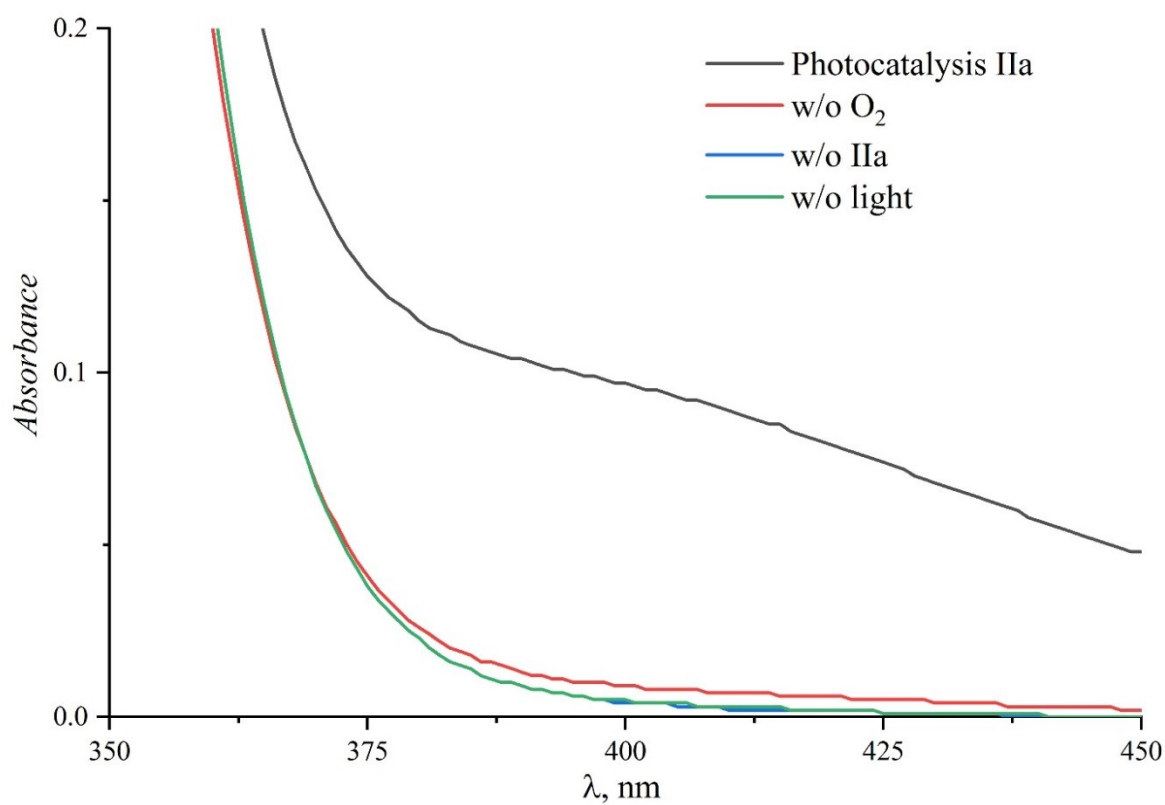
Figure SI11. Cyclic voltammogram of TEMPOL (c 1.0 mM in 0.1 M DMF solution of $LiClO_4$).
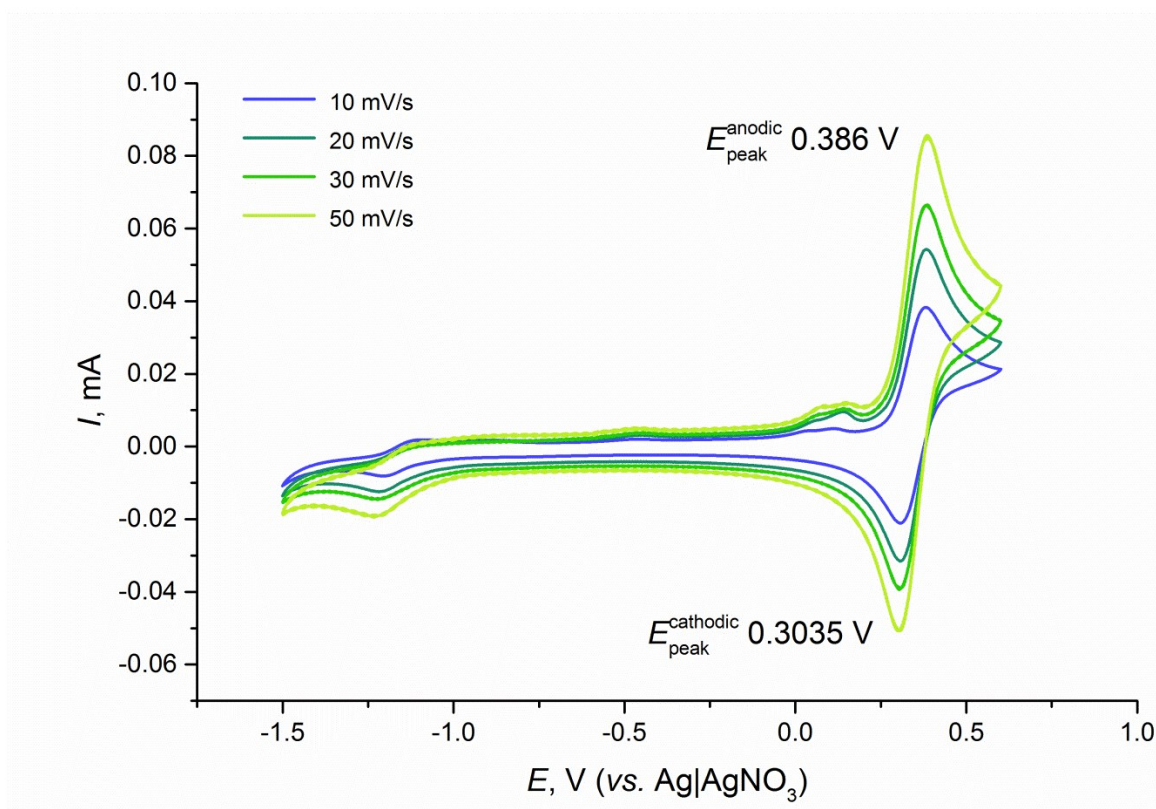
Figure SI12. Cyclic voltammogram of **IIa** (c 1.0 mM in 0.1 M DMF solution of $LiClO_4$) in -1.5 – 0 V potential range.
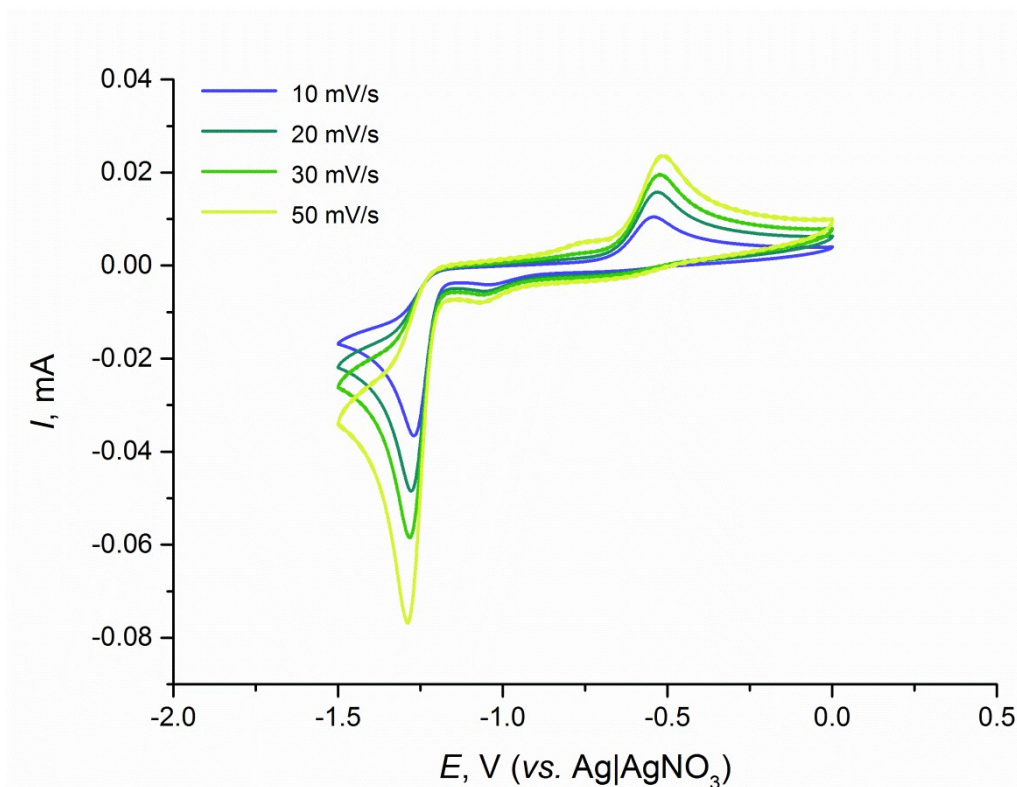
Figure SI13. Cyclic voltammogram of **IIa** (*c* 1.0 mM in 0.1 M DMF solution of LiClO₄) in -1.0 – +0.6 V potential range.
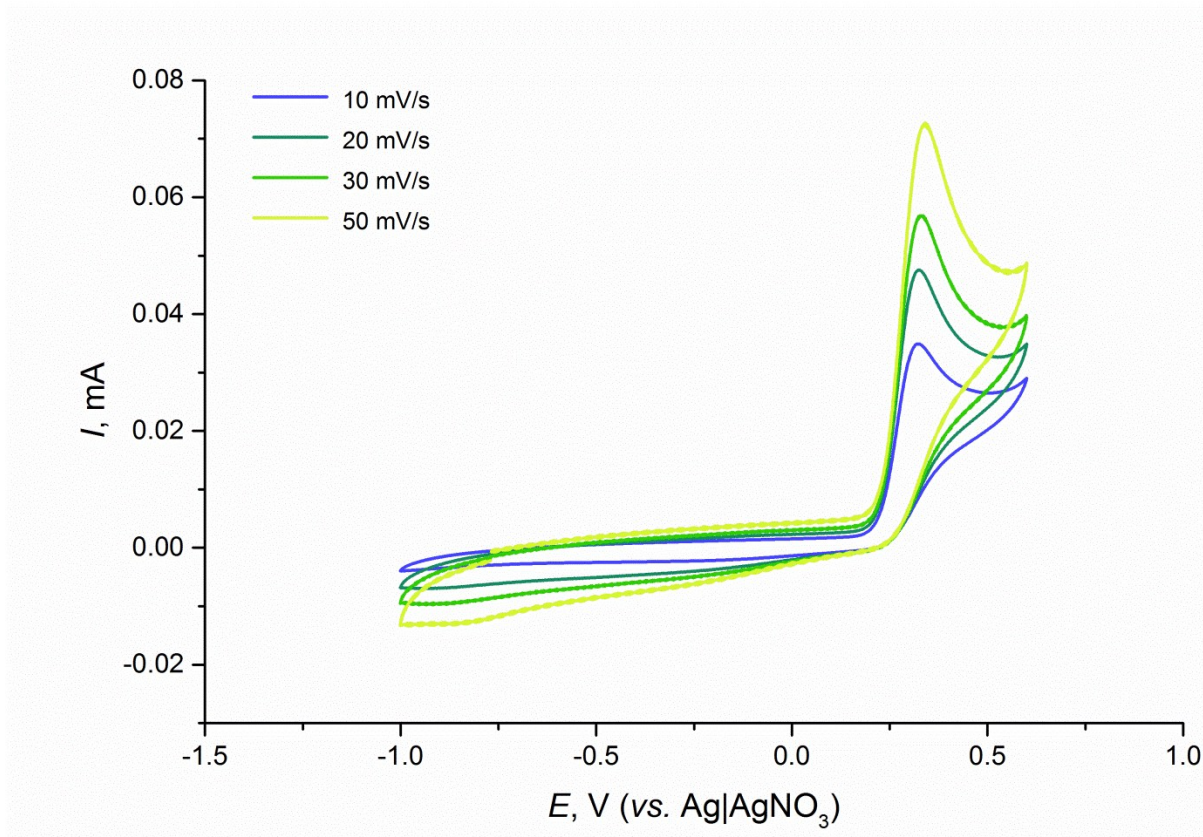
Figure SI14. Emission spectrum in the near IR range (no emission of the singlet oxygen).
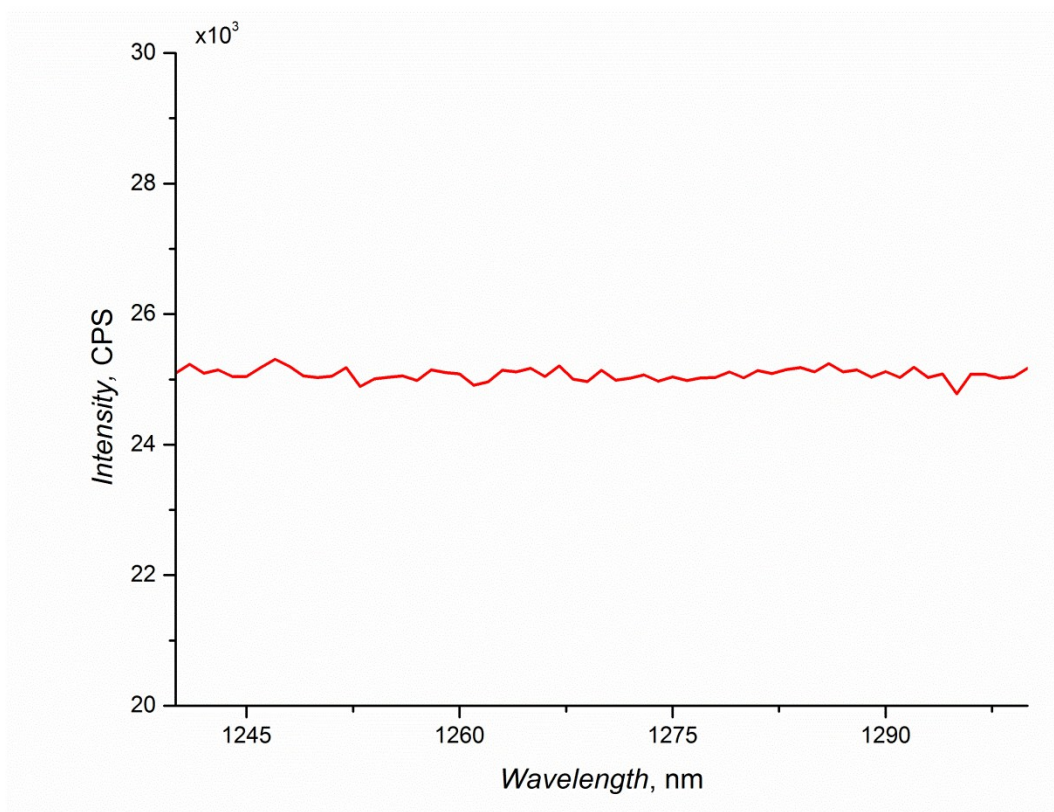
Figure SI15a. Emission spectra of compound **IIa** (water, *c* 0.1 mM) in the presence of oxalate ions.
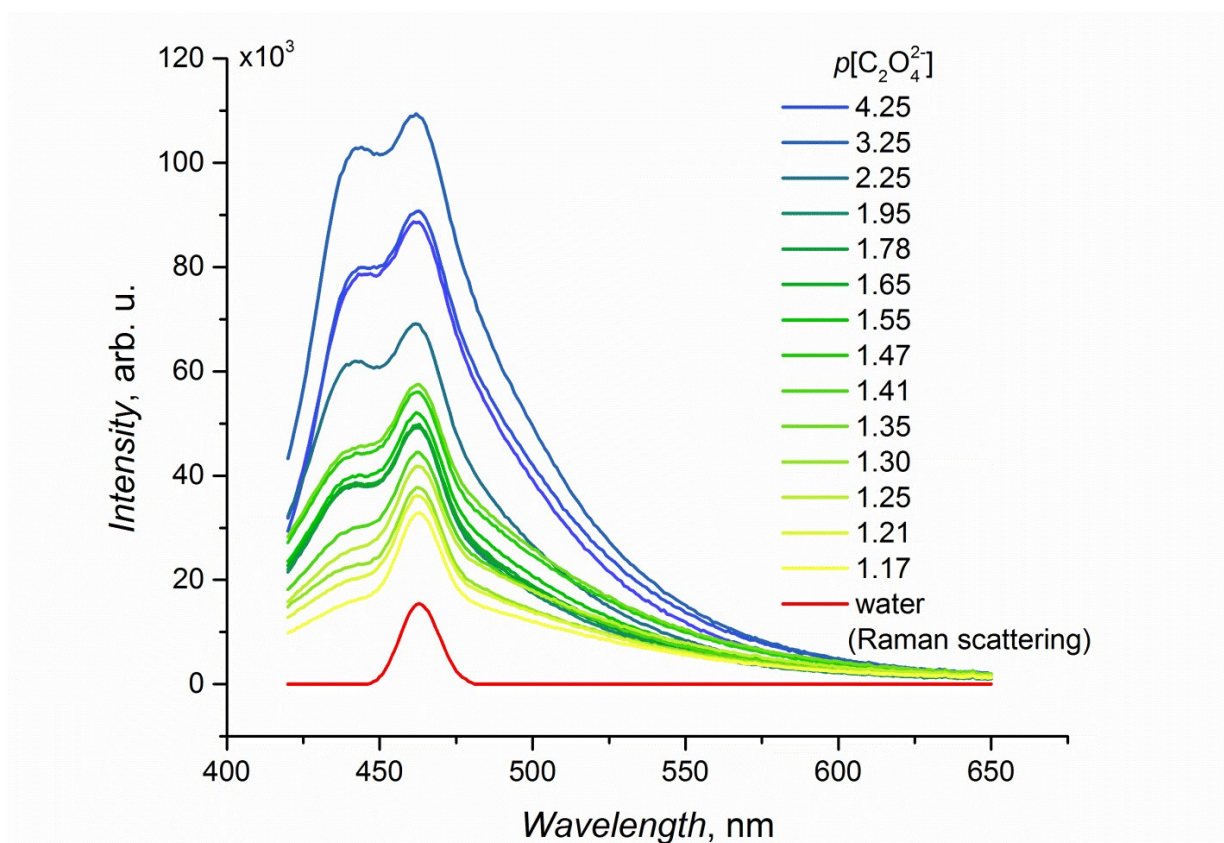
Figure SI16. Stern-Volmer plot for fluorescence intensity of compound **IIa** (water, *c* 0.1 mM) at variable concentrations of oxalate ions.
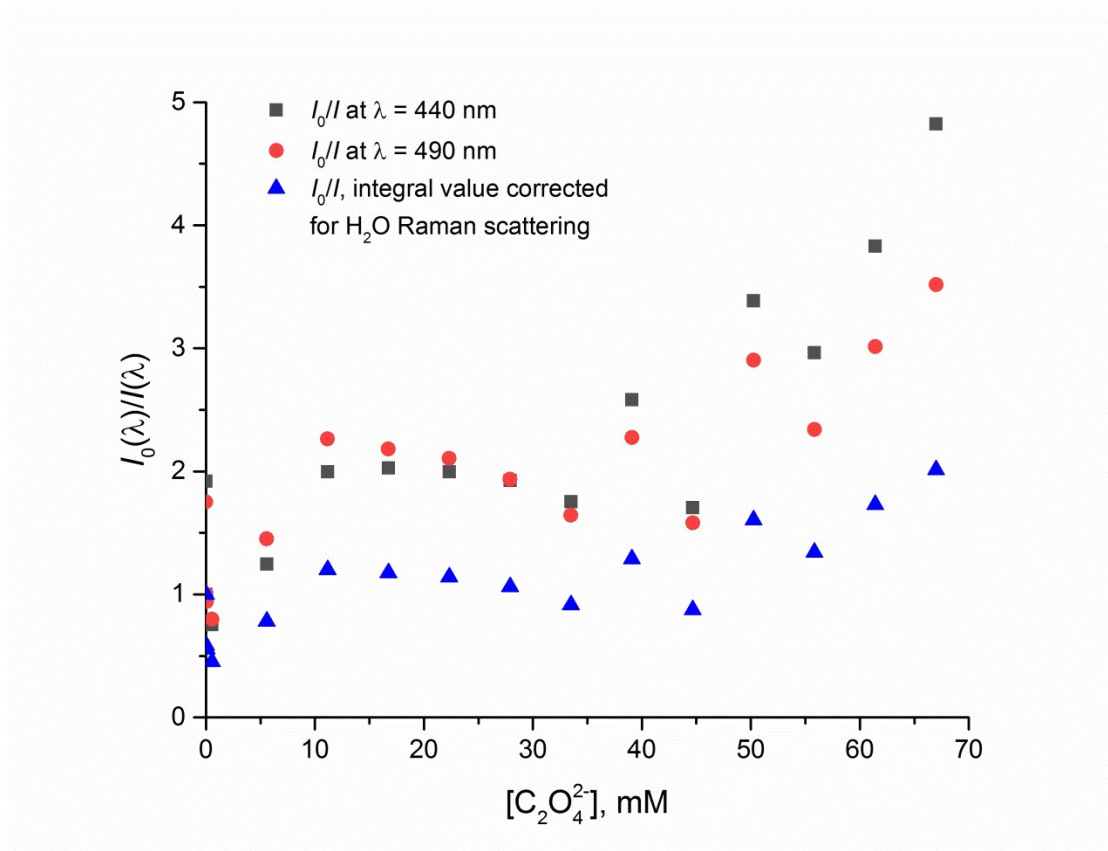
Figure SI17. Dependence of fluorescence kinetics of compound **IIa** on the concentration of oxalate ions.
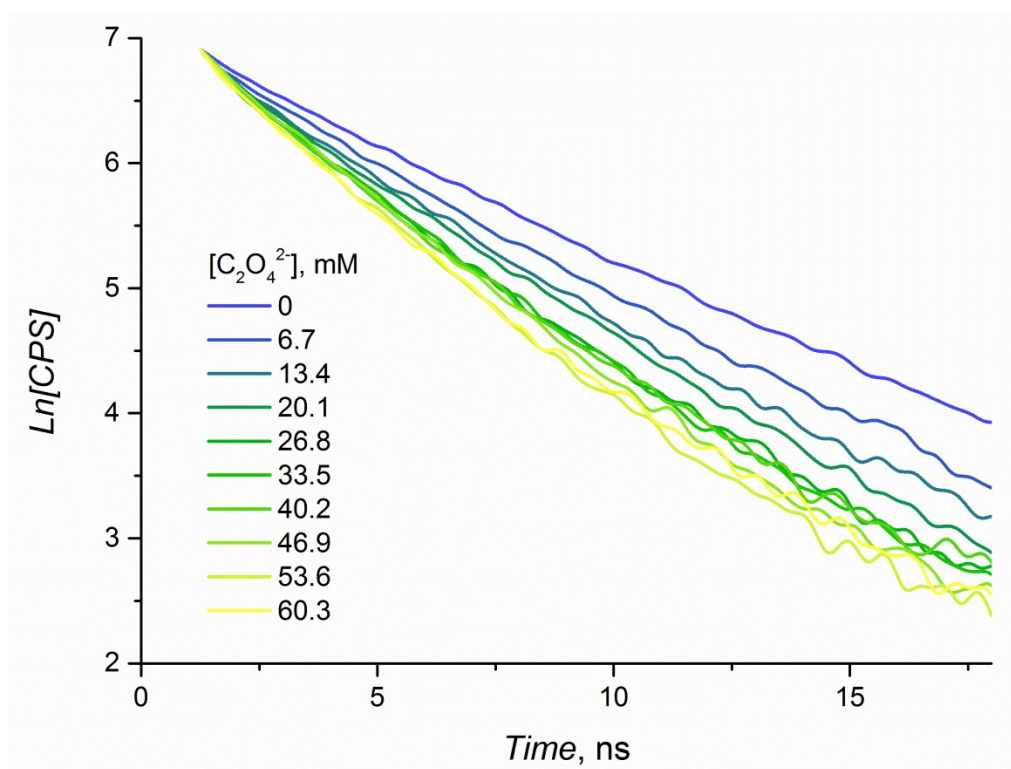
Figure SI18. Dependence of fluorescence kinetics of compound **IIa** on the concentration of oxygen.
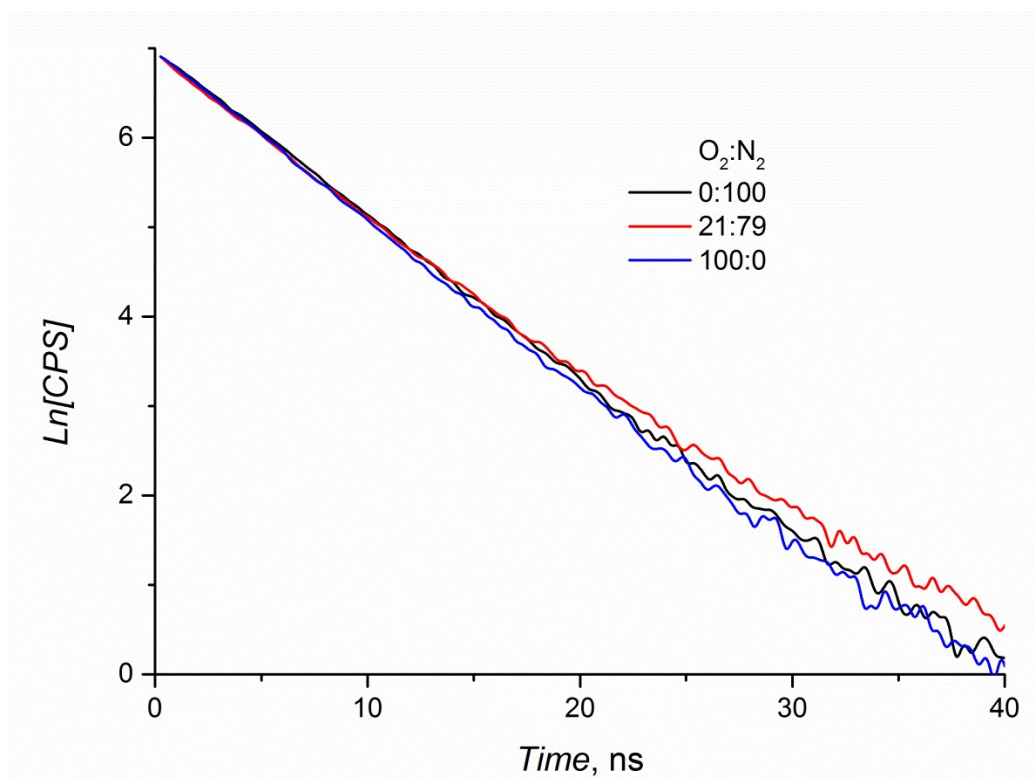
Figure SI19. 3D plot of excitation/emission spectra of *N*-methylisoquinolinium tetrafluoroborate (*c* 0.01 mM) in water.
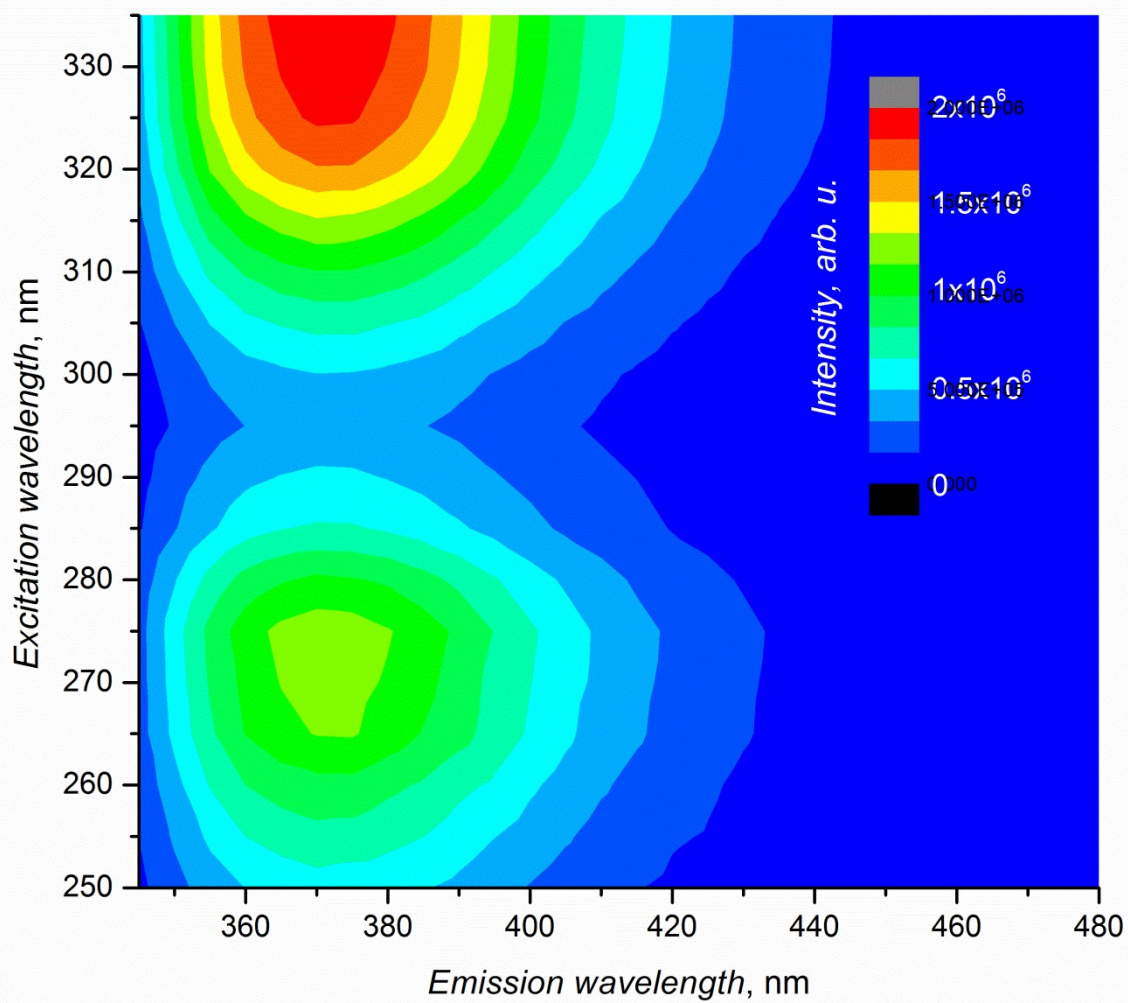
Computational Details

All calculations were performed by using the Gaussian 16 suite of quantum chemical programs[i] at Resource center "Computer center of Saint Petersburg State University". Geometry optimizations of molecules were performed with the B3LYP density functional method[ii] and 6-31+G(d,p) basis set with PCM solvation model for water. Stationary points on the respective potential-energy surfaces were characterized at the same level of theory by evaluating the corresponding Hessian indices.

Table SI1. Absolute Energies (au) and Cartesian Coordinates of the stationary point for **IIa**.
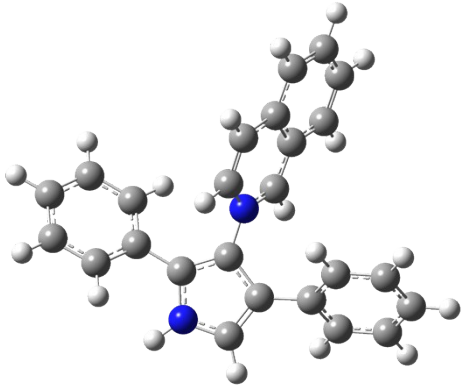
E = -1073.536870, **H (0K)** = -1073.163207,
**H (298K)** = -1073.141757,
G (298K) = -1073.214487au.
Number of imaginary frequency = 0

C	2.6316420	4.0257350	-1.2111210	C	-3.1874310	0.5156370	-0.8251850
C	2.1888090	2.7385590	-1.4162940	C	-5.4302070	-0.5417620	0.4638040
C	1.2827110	2.1535210	-0.4883820	H	-4.1523460	-2.1721500	1.0388560
C	0.8340800	2.9027690	0.6491020	C	-4.3976950	1.2111420	-0.8425900
C	1.3099560	4.2237910	0.8295960	H	-2.3319530	0.9202110	-1.3560170
C	2.1899940	4.7683470	-0.0845950	C	-5.5233900	0.6852970	-0.2007740
H	1.0811790	0.2402370	-1.5175440	H	-6.2974370	-0.9559190	0.9691850
H	3.3230880	4.4803680	-1.9125000	H	-4.4629930	2.1584720	-1.3692030
H	2.5209160	2.1628480	-2.2740110	H	-6.4647000	1.2260470	-0.2193540
C	0.7994470	0.8477980	-0.6665520	C	1.8440510	-2.2758100	0.0636780
C	-0.0702580	2.2691910	1.5437560	C	2.5917110	-3.0875630	-0.8097310
H	0.9760950	4.7971590	1.6882360	C	2.5289720	-1.5581490	1.0618910
H	2.5523120	5.7816300	0.0563700	C	3.9793230	-3.1836420	-0.6842910
C	-0.4883090	0.9892510	1.3189910	H	2.0818080	-3.6354260	-1.5967390
H	-0.4293490	2.7918040	2.4230300	C	3.9181960	-1.6467480	1.1792170
H	-1.1542870	0.4490490	1.9764910	H	1.9739560	-0.9465370	1.7668220
C	-0.4783350	-3.2854180	-0.2483100	C	4.6491780	-2.4602310	0.3079100
C	0.3733180	-2.2090830	-0.0618270	H	4.5374140	-3.8163450	-1.3683400
C	-0.4866490	-1.0643150	0.0095050	H	4.4269210	-1.0870570	1.9586780
C	-1.8141470	-1.4627910	-0.1307800	H	5.7287850	-2.5300950	0.4013380
H	-0.2563200	-4.3380330	-0.3348890	N	-0.0524730	0.2910460	0.2065430
C	-3.0810770	-0.7155340	-0.1523190	N	-1.7680320	-2.8268030	-0.2744470
C	-4.2190850	-1.2350080	0.4938880	H	-2.5783790	-3.4058770	-0.4465980

Figure SI20. Calculated UV-Vis spectrum of **IIa**.

Excitation energies and oscillator strengths for two lowest electronically excited singlet states (TD DFT, B3LYP/6-31+g(d,p), water /PCM)

Excited State   1: 2.5638 eV, 483.60 nm, f=0.0271, HOMO -> LUMO 99.6%

Excited State   2: 3.2606 eV, 380.25 nm, f=0.0535, HOMO-1 -> LUMO   97.4%

UV-Vis Spectrum
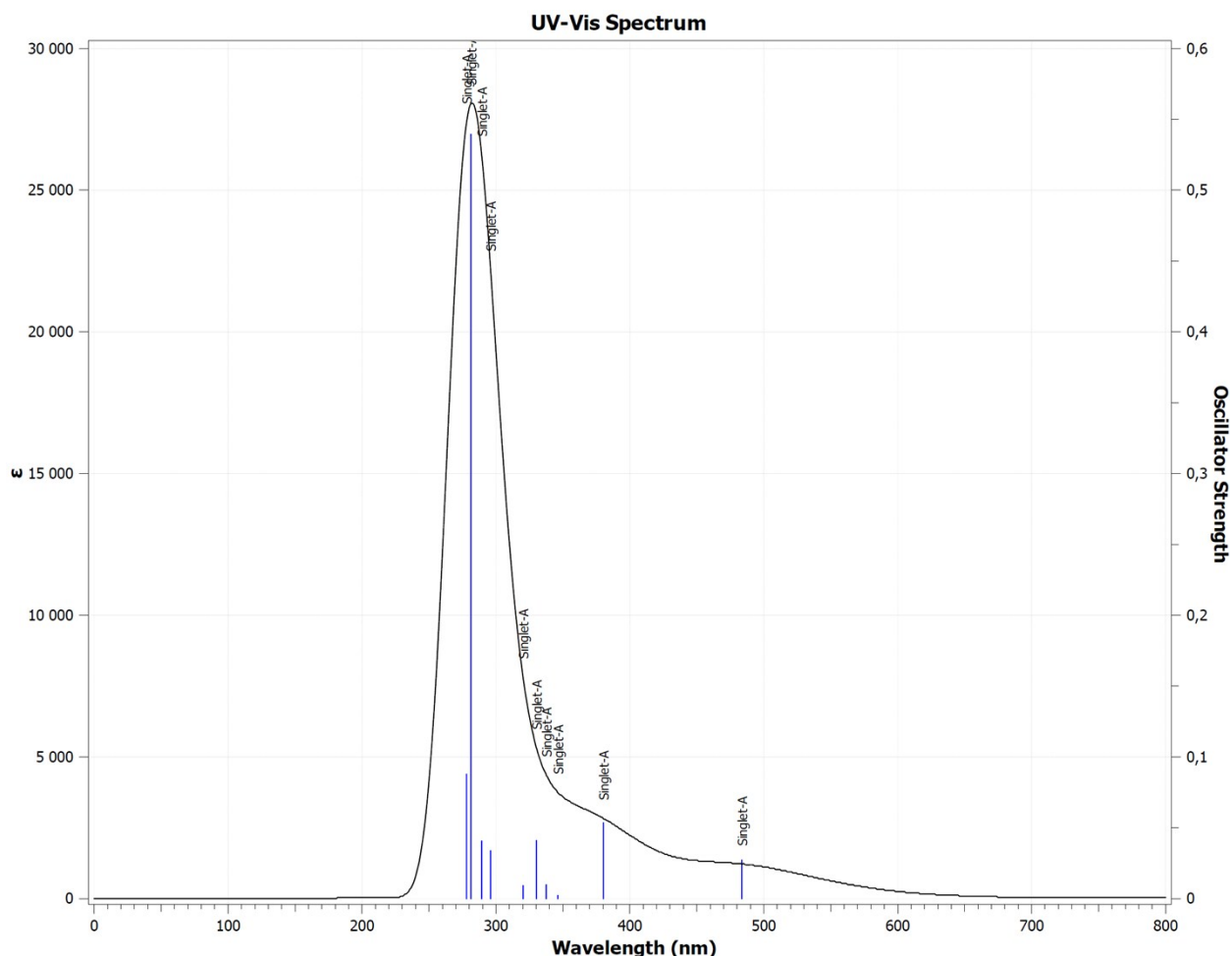
[i] Gaussian 16, Revision A.03, Frisch, M. J.; Trucks, G. W.; Schlegel, H. B.; Scuseria, G. E.; Robb, M. A.; Cheeseman, J. R.; Scalmani, G.; Barone, V.; Petersson, G. A.; Nakatsuji, H.; Li, X.; Caricato, M.; Marenich, A. V.; Bloino, J.; Janesko, B. G.; Gomperts, R.; Mennucci, B.; Hratchian, H. P.; Ortiz, J. V.; Izmaylov, A. F.; Sonnenberg, J. L.; Williams-Young, D.; Ding, F.; Lipparini, F.; Egidi, F.; Goings, J.; Peng, B.; Petrone, A.; Henderson, T.; Ranasinghe, D.; Zakrzewski, V. G.; Gao, J.; Rega, N.; Zheng, G.; Liang, W.; Hada, M.; Ehara, M.; Toyota, K.; Fukuda, R.; Hasegawa, J.; Ishida, M.; Nakajima, T.; Honda, Y.; Kitao, O.; Nakai, H.; Vreven, T.; Throssell, K.; Montgomery, J. A., Jr.; Peralta, J. E.; Ogliaro, F.; Bearpark, M. J.; Heyd, J. J.; Brothers, E. N.; Kudin, K. N.; Staroverov, V. N.; Keith, T. A.; Kobayashi, R.; Normand, J.; Raghavachari, K.; Rendell, A. P.; Burant, J. C.; Iyengar, S. S.; Tomasi, J.; Cossi, M.; Millam, J. M.; Klene, M.; Adamo, C.; Cammi, R.; Ochterski, J. W.; Martin, R. L.; Morokuma, K.; Farkas, O.; Foresman, J. B.; Fox, D. J. Gaussian, Inc., Wallingford CT, **2016**.

[2] (a) Becke, A. D. *J. Chem. Phys.* **1993**, *98*, 5648–5652. (b) Becke, A. D. *Phys. Rev. A* **1988**, *38*, 3098–3100. (c) Lee, C.; Yang, W.; Parr, R. G. *Phys. Rev. B* **1988**, *37*, 785–789.